


 Cite this: *RSC Adv.*, 2020, **10**, 25780

# Preparative separation of mangiferin glycosides by high speed counter current chromatography and comparison of their antioxidant and antitumor activities†

 Tingting Xu<sup>a</sup> and Xueming Wu<sup>id</sup>\*<sup>b</sup>

Mangiferin, a xanthonoid with various bioactivities. The low solubility of mangiferin limits the use in pharmacological fields. In this study, high-speed counter-current chromatography (HSCCC) was used to separate and purify mangiferin glycosides from the crude sample after enzymatic glycosylation of mangiferin. Two fructosyl mangiferin were successfully purified by HSCCC with a two-phase-solvent system composed of *n*-butanol–methanol–water (6 : 1 : 6, v/v). A total of 18 mg of mangiferin (I), 73 mg of β-D-fructofuranosyl-(2 → 6)-mangiferin (II), and 58 mg of β-D-diffructofuranosyl-(2 → 6)-mangiferin (III) were obtained in one-step separation from 150 mg of the crude sample with purities of 99.2%, 98.7% and 98.9%, respectively. The chemical structures were identified by HRMS, <sup>1</sup>H-NMR, <sup>13</sup>C-NMR and 2D NMR. Mangiferin glycosides showed higher antioxidant and antitumor activities compared to that of mangiferin by employing DPPH scavenging effect, reducing power and cytotoxicity assay. Therefore, these novel fructosyl mangiferin exhibit a great potential to be developed into new medicines.

Received 14th May 2020

Accepted 1st July 2020

DOI: 10.1039/d0ra04307a

[rsc.li/rsc-advances](http://rsc.li/rsc-advances)

## 1. Introduction

Mangiferin is a xanthone glucoside present in many plant species including Iridaceae, Gentianaceae and Anacardiaceae, while it was originally isolated from *Mangifera indica* L.<sup>1</sup> The functional groups of mangiferin have several aromatic and non-aromatic secondary hydroxyl groups, one primary glycosidic hydroxyl group and one lactonic carbonyl group.<sup>2</sup> Owing to these functional groups, it shows multiple pharmacological activities, including the anti-oxidant,<sup>3,4</sup> central nervous system-stimulating,<sup>5</sup> analgesic,<sup>6</sup> antitumor,<sup>7</sup> antidiabetic<sup>8</sup> and anti-inflammation.<sup>9</sup> However, the solubility of mangiferin is a serious issue which limits its pharmacological uses. Glycosylation has been used to improve the solubility and bioactivity of many natural products.<sup>10</sup> These glycosylation reactions in water are not efficient with lower yields due to the serious solubility issue of the acceptor.<sup>11</sup> Enzymatic glycosylation in organic solvents supply numerous industrially attractive advantages, such as reversing of the thermodynamic equilibrium of hydrolysis reactions, increasing the solubility of hydrophobic substrates, and eliminating of microbial contamination. Screening and exploiting of organic solvent-stable

glycosidases have been studied to improve the stability of enzymes while catalysing reactions in organic solvents.<sup>12</sup> In our previous study, we developed an effective method to enzymatic synthesis of mangiferin glycosides in hydrophilic organic solvents, high concentrations and high yields of mangiferin glycosides were achieved in a low-cost process.<sup>13</sup> However due to the structural similarity of the glycosylated mangiferin, it was difficult to directly separate and purify an enough amount of product from the crude sample by single chromatographic method.

High speed counter-current chromatography (HSCCC), a liquid–liquid separation chromatographic technology, has been widely applied for the large-scale separation of chemical compositions and biotransformation reactor.<sup>14,15</sup> It provides unique advantages such as larger loading capacity and higher sample recovery compared to traditional techniques.<sup>16,17</sup> For these reasons, HSCCC has been used to purify mangiferin from mango fruit peel, the ethyl acetate–*n*-butanol–water (4 : 1 : 5) solvent system showed ideal *k* value of 1.76 for mangiferin.<sup>18</sup> Genistein and daidzein were separated for the first time from *Hericium erinaceum* mycelium using chloroform–dichloromethane–methanol–water (4 : 2 : 3 : 2) solvent system.<sup>19</sup> Four glycosides from *Gentianae radix* have been efficiently purified using different solvent systems.<sup>20</sup> To the best of our knowledge, no report has been published on the use of HSCCC for one-step purification of mangiferin glycosides. The aims of this study, therefore, were to isolate and purify two types of mangiferin

<sup>a</sup>School of Medicine & Holistic Integrative Medicine, Nanjing University of Chinese Medicine, Nanjing, 210023, China

<sup>b</sup>School of Pharmacy, Nanjing University of Chinese Medicine, Nanjing, 210023, China. E-mail: xuemingwu@njucm.edu.cn; Tel: +86 25 8581 1516

† Electronic supplementary information (ESI) available: The HRMS and NMR spectroscopic data for compounds II and III. See DOI: 10.1039/d0ra04307a



glycosides with high purity using HSCCC, and evaluate their antioxidant and antitumor activities.

## 2. Materials and methods

### 2.1 Materials and reagents

Mangiferin was purchased from Zelang (Jiangsu, China). 2,2-Diphenyl-1-picrylhydrazyl (DPPH) was obtained from Sigma (St. Louis, MO, USA). Methanol used for HPLC analysis was of chromatographic grade from Sinopharm (Shanghai, China). *n*-Butanol, ethyl acetate, hexane, methanol used for HSCCC separation were of analytical grade and purchased from Beijing Chemical Factory (Beijing, China). Water used for deionized by an osmosis Milli-Q system (Millipore, USA). All other chemicals were of analytical grade and purchased from Sunshine (Nanjing, China).  $\beta$ -Fructofuranosidase was purified from *Arthro-bacter nicotianae* XM6 (CCTCC M2010164).

### 2.2 Apparatus

HSCCC was performed with a model TBE-300B high speed counter current chromatography (Tauto Biotech, Shanghai, China). The instrument was equipped with three multilayer coil separation columns connected in series (diameter of tube = 2.6 mm, total volume = 300 mL, the range of  $\beta$  values = 0.5–0.8) and a 20 mL sample loop. The revolution speed of the apparatus was adjustable, ranging from 0 to 1000 rpm. An HX 1050 constant-temperature circulator (Beijing Boyikang Lab Instrument Company, Beijing, China) was used to control separation temperature. Sepu 3000 chromatography workstation (Hangzhou Puhui Science Apparatus Co. Ltd., Hangzhou, China) was employed to record the chromatograms.

### 2.3 Enzymatic glycosylation of mangiferin

The glycosylation reaction (3.0 L) was conducted in 1/15 M  $\text{Na}_2\text{HPO}_4/\text{KH}_2\text{PO}_4$  buffer (pH 6.47) containing 0.24 U  $\text{mL}^{-1}$   $\beta$ -fructofuranosidase, 20% (w/v) sucrose and 60 mM mangiferin and 15% (v/v) dimethyl sulfoxide (DMSO). The reaction mixture was conducted at 35 °C with shaking at 180 rpm for 12 h, then the reaction was stopped at 100 °C for 5 min.<sup>13</sup>

### 2.4 Preparation of crude sample

After the reaction solution has been loaded on AB-8 macroporous resin column (80 cm  $\times$  3 cm), the column was eluted by 3 L of distilled water (pH 4.0) acidified with acetic acid to remove sucrose, and then was eluted by 1 L of 100% ethanol. The 100% ethanol fraction was collected and evaporated to dryness by rotary evaporation at 60 °C under reduced pressure.

### 2.5 Selection of the two-phase solvent systems

The selection of two-phase solvent system was based on the partition coefficient ( $k$ ) of the target components, which can be determined by HPLC. 10 mg of sample was dissolved with 5 mL of the upper and lower phases of the solvent system, and the sample was mixed thoroughly. After partition equilibration, the upper phase and the lower phase solution was taken for HPLC

analysis, respectively. The  $k$  value was defined as the peak area of component in the upper phase ( $A_U$ ) divided by that of in the lower phase ( $A_L$ ) ( $k = A_U/A_L$ ).

### 2.6 Preparation of two-phase solvent system and sample solution

In the present study, *n*-butanol–methanol–water (6 : 1 : 6, v/v/v) was used as the two-phase solvent system for HSCCC separation. It was prepared by adding all the solvents to a separatory funnel according to the volume ratios and fully equilibrated. Then, the upper and lower phase were separated and degassed for 40 min shortly before using. The sample solution was prepared by dissolving 150 mg of crude sample into 10 mL of the lower phase of the selected solvent system.

### 2.7 HSCCC separation procedure

First, the multilayer coil column was entirely filled with the lower phase as the stationary phase. Then the upper phase as the mobile phase was pumped into the column at a flow rate of 1.0  $\text{mL min}^{-1}$  during rotation. The apparatus was rotated at 850 rpm. After the hydrodynamic equilibrium was reached, 150 mg prepared sample solution was loaded into the column through the injection valve. The effluent from the outlet of the column was continuously monitored with a UV detector at 254 nm. Each peak fraction was manually collected according to the chromatographic peak profiles displayed on the recorder. After running, the solvents in the column were pushed out and the retention of stationary phase was measured.

### 2.8 Analysis and identification of HSCCC peak fractions

The crude sample, each fraction obtained by HSCCC were performed on Dionex P680A HPLC system. The analysis was performed in a Discovery ODS C18 column (250 mm  $\times$  4.6 mm, i.d., 5  $\mu\text{m}$ ) at 30 °C. Methanol/0.1% formic acid (v/v) was used as the mobile phase in gradient elution mode as follows: 0–20 min, 20–60% methanol.<sup>13</sup> The effluent was monitored at 316 nm and the flow rate was 1  $\text{mL min}^{-1}$ . The molecular weight of each fraction was carried out on a TOF mass spectrometer (Micromass) equipped with an electrospray ion source was used in positive-ion mode. <sup>1</sup>H, <sup>13</sup>C and 2D NMR spectra of each fraction were obtained using a Bruker AV-500 spectrometer (Switzerland), operating at 500 MHz. Samples were dissolved in  $\text{DMSO-}d_6$  at room temperature with tetramethylsilane as the chemical shift reference.

### 2.9 Evaluation of antioxidant activity

The effects of reference control (ascorbic acid), mangiferin,  $\beta$ -D-fructofuranosyl-(2  $\rightarrow$  6)-mangiferin (Mangiferin-F) and  $\beta$ -D-fructofuranosyl-(2  $\rightarrow$  6)-mangiferin (Mangiferin-F2) on the 2,2-diphenyl-1-picrylhydrazyl (DPPH) radical were estimated according to the method of Singh.<sup>21</sup> Briefly, 150  $\mu\text{L}$  of various concentration samples (6.25, 12.5, 25, 50, 100 and 250  $\mu\text{M}$ ) were mixed with 150  $\mu\text{L}$  of 150  $\mu\text{M}$  DPPH solution. After being incubated at 37 °C for 30 min, the absorbance of the mixture was measured at 517 nm. The free radical scavenging activity of the reaction solution was calculated as a percentage of DPPH



discolouration using the following equation: Radical scavenging activity (%) =  $(1 - A_{\text{sample}}/A_{\text{control}}) \times 100$ , where  $A_{\text{sample}}$  is the absorbance of the solution when the sample has been added at a particular level, and  $A_{\text{control}}$  is the absorbance of the DPPH solution. The results were expressed as mean values  $\pm$  standard deviations ( $n = 8$ ).

The reducing power of mangiferin, mangiferin-F, mangiferin-F2 and ascorbic acid was determined according to the method of Sakariah<sup>22</sup> with some modifications. Mixtures of 50  $\mu\text{L}$  different concentrations of mangiferin, mangiferin-F, mangiferin-F2 and ascorbic acid, 50  $\mu\text{L}$  of phosphate buffer (0.2 M, pH 6.6), and 50  $\mu\text{L}$  of 1% potassium ferricyanide were prepared and incubated at 37  $^{\circ}\text{C}$  for 20 min. Next, 50  $\mu\text{L}$  of 10% trichloroacetic acid was added to the mixtures, followed by centrifuging at 4000 rpm for 10 min. The supernatant (200  $\mu\text{L}$ ) was mixed with 50  $\mu\text{L}$  of distilled water and 30  $\mu\text{L}$  of 0.1% ferric chloride and the absorbance was measured at 700 nm after standing for 10 min. Higher absorbance of the reaction mixture indicated higher reducing power of the samples. The results were expressed as mean values  $\pm$  standard deviations ( $n = 8$ ).

### 2.10 Cell growth and maintenance

Human leukemia promyelocytic cells HL60, and human papillary thyroid cancer cells TPC1 were purchased from the Institute of Biochemistry and Cell Biology, Chinese Academy of Sciences (Shanghai, China). Two cells were cultured in RPMI-1640 with FBS (10%), 2 mM glutamine, 100 U  $\text{mL}^{-1}$  penicillin, and 100  $\mu\text{g mL}^{-1}$  streptomycin at 37  $^{\circ}\text{C}$  in a humidified incubator with 5%  $\text{CO}_2$ .

### 2.11 MTT assay

The cytotoxicity effects of mangiferin-F, mangiferin-F2 and mangiferin were analyzed using MTT assay.<sup>23</sup> Approximately  $2 \times 10^4$  cells suspended in 100  $\mu\text{L}$  of growth medium were added to each well of a 96 well plates and were incubated. The cells were treated with mangiferin, mangiferin-F and mangiferin-F2 at final concentrations of 5, 10, 20, 40, 80, 160, 250  $\mu\text{M}$  for 48 h. Cells treated with dimethyl sulfoxide (DMSO) alone (0.01%) were used as control. Each concentration was tested with 6 replicate wells. After 48 h, the medium containing the treatments was removed, and 100  $\mu\text{L}$  of MTT solution (0.5 mg  $\text{mL}^{-1}$ ) was added to each well and incubated at 37  $^{\circ}\text{C}$  for 3 h. The formazan crystals were dissolved in 100  $\mu\text{L}$  of DMSO, and the absorbance was measured at 490 nm with ELISA plate reader. The experiment was performed in triplicate.

Table 1  $k$  values of the target compounds in two-phase solvent systems

Solvent system	Volume ratio (v/v)	$k_{\text{I}}$	$k_{\text{II}}$	$k_{\text{III}}$
<i>n</i> -Butanol–water	1 : 1	3.89	0.92	0.23
Ethyl acetate–water	1 : 1	0.15	0.05	0.01
Hexane–methanol–water	1 : 1 : 1	0.05	0.01	0.001
<i>n</i> -Butanol–methanol–water	6 : 1 : 6	2.10	1.48	0.75
<i>n</i> -Butanol–ethyl acetate–water	5 : 1 : 6	2.50	1.21	0.64

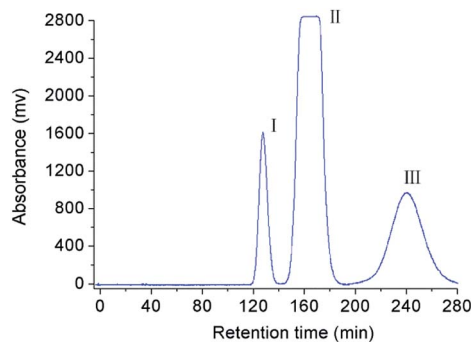


Fig. 1 HSCCC chromatogram of crude sample under the optimized condition. Solvent systems: *n*-butanol–methanol–water (6 : 1 : 6, v/v); stationary phase: lower phase; flow rate: 1  $\text{mL min}^{-1}$ ; revolution speed: 850 rpm; sample amount: 150 mg; separation temperature: 25  $^{\circ}\text{C}$ ; detection wavelength: 254 nm.

## 3. Results and discussion

### 3.1 Selection of the two-phase solvent systems

The selection of a suitable two-phase solvent system is a crucial step in a HSCCC separation, which can provide the ideal partition coefficient ( $k$ ) for each target compound. As previously reported, the  $k$  value should be in range of 0.5–2 to get a short elution time and a good resolution.<sup>24</sup> The small  $k$  value usually results in poor separation resolution, while large  $k$  value tends to produce broader chromatographic peaks due to a longer elution time.

For separation of mangiferin and fructosyl mangiferins, a series of experiments were performed to optimize the two-

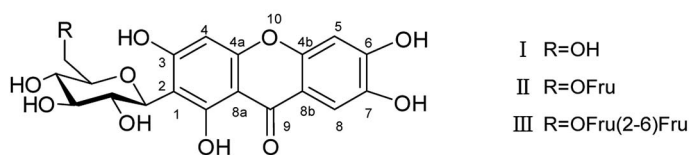
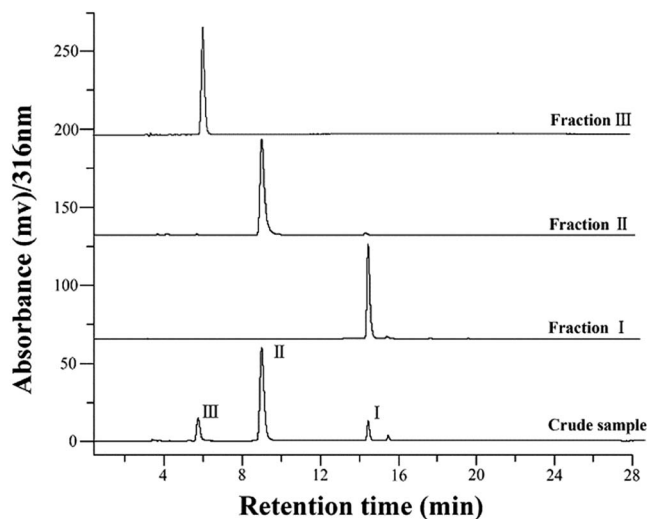


Fig. 2 HPLC analysis and chemical structures of compounds separated by HSCCC.



Table 2  $^1\text{H}$  and  $^{13}\text{C}$ -NMR data for mangiferin and its glucosides ( $\delta$  in ppm,  $J$  in Hz)

No	Mangiferin		$\beta$ -D-Fructofuranosyl-(2 $\rightarrow$ 6)-mangiferin		$\beta$ -D-Difructofuranosyl-(2 $\rightarrow$ 6)-mangiferin	
	$^{13}\text{C}$ NMR ( $\delta_{\text{C}}$ )	$^1\text{H}$ NMR $\delta_{\text{H}}$ (J/Hz)	$^{13}\text{C}$ NMR ( $\delta_{\text{C}}$ )	$^1\text{H}$ NMR $\delta_{\text{H}}$ (J/Hz)	$^{13}\text{C}$ NMR ( $\delta_{\text{C}}$ )	$^1\text{H}$ NMR $\delta_{\text{H}}$ (J/Hz)
1	161.7	13.75 (s, 1-OH)	161.7	13.75 (s, 1-OH)	161.7	13.75 (s, 1-OH)
2	107.6		107.4		107.3	
3	163.8	10.52 (s, 3-OH)	163.8		163.7	
4	93.3	6.37 (s)	93.4	6.36 (s)	93.4	6.37 (s)
4a	156.2		156.3		156.3	
4b	150.7		150.8		150.8	
5	102.6	6.86 (s)	102.6	6.86 (s)	102.6	6.86 (s)
6	153.9	10.63 (s, 6-OH)	154.1		154.1	
7	143.7	9.74 (s, 7-OH)	143.7		143.7	
8	108.1	7.38 (s)	108.1	7.38 (s)	108.1	7.38 (s)
8a	111.7		111.7		111.7	
8b	101.3		101.3		101.4	
9	179.0		179.1		179.1	
1'	73.1	4.60 (d, 9.8)	73.1	4.59 (d, 9.8)	73.2	4.60 (d, 9.8)
2'	70.2	4.04 (t, 17.7)	70.2	3.98 (t)	70.3	4.00 (m)
3'	78.9	3.12–3.23 (m)	78.7	3.21 (m)	78.3	3.22 (m)
4'	70.6		70.7	3.21 (m)	70.8	3.20 (m)
5'	81.5		75.2	3.79 (t, 15.2)	75.2	3.74–3.82 (m)
6'	61.5	3.70 (d, 11.3), 3.40–3.43 (H, m)	62.4	3.42, 3.52 (2H, m)	62.9	3.51, 3.72 (2H, m)
1''			61.3	3.30–3.40 (2H, m)	60.9	3.28, 3.40 (2H, m)
2''			104.2		104.3	
3''			79.6	3.30 (1H, m)	80.3	3.59 (m)
4''			76.7	3.94 (t, 14.5)	76.5	3.92–3.99 (m)
5''			82.1	3.52 (1H, m)	75.7	3.74–3.82 (m)
6''			61.9	3.88, 3.58 (2H, m)	62.5	3.42, 3.51 (2H, m)
1'''					61.3	3.26–3.37 (2H, m)
2'''					104.2	
3'''					79.6	3.30 (m)
4'''					76.3	3.92–3.99 (m)
5'''					82.0	3.53 (m)
6'''					62.2	3.51, 3.84 (2H, m)

phase solvent system for HSCCC separation. The  $k$  values of the target compounds were described in Table 1. The results shown that the solvent systems composed of ethyl acetate–water (1 : 1, v/v) and hexane–methanol–water (1 : 1 : 1, v/v/v) had too small  $k$  values for all compounds indicating poor resolution. The solvent system of *n*-butanol–water (1 : 1, v/v) gave large  $k$  value for compound **I** and small  $k$  value for compound **III**. So, the solvent system of *n*-butanol–water (1 : 1, v/v) was slightly modified. When *n*-butanol–ethanol–water (6 : 1 : 6, v/v/v) and *n*-butanol–ethyl acetate–water (5 : 1 : 6, v/v/v) were used as the two-phase solvent system, the  $k$  values of target compounds were suitable. Finally, the solvent system of *n*-butanol–methanol–water (6 : 1 : 6, v/v) was used to isolate the target compounds with best suitable  $k$  values ( $k_{\text{I}} = 2.10$ ,  $k_{\text{II}} = 1.48$  and  $k_{\text{III}} = 0.75$ ). Based on previous researches, low flow rate and high revolution speed could both lead to increase the retention of the stationary phase.<sup>19,25</sup> The flow rate of 1 mL min<sup>-1</sup>, and the retention speed of 850 rpm were selected as the suitable conditions to run the HSCCC separation. Under the optimized conditions, the retention of stationary phase was 56%, and the purified compounds **I**, **II** and **III** were obtained (Fig. 1). About 18 mg of compound **I**, 73 mg of

compound **II**, and 58 mg of compound **III** were obtained from 150 mg of crude sample. As shown in Fig. 2, the purities of compounds **I**, **II** and **III** were 99.2%, 98.7%, and 98.9%, respectively.

### 3.2 Identification of chemical structure

The chemical structure of compounds **II** and **III** was identified by HRMS and NMR spectra. The high-resolution ESI mass spectrum of compounds **II** showed an ion peak  $[\text{M}-\text{H}]^-$  at  $m/z$  583.1324 (calculated for  $\text{C}_{25}\text{H}_{27}\text{O}_{16}$ , 583.1299) (Fig. S11-a†). Compared with mangiferin, the compound **II** has an additional formula  $\text{C}_6\text{H}_{10}\text{O}_5$ , suggesting that compound **II** may be a mangiferin monosaccharide derivative. The  $^1\text{H}$ -NMR spectra in low field showed three ethylenic signals [ $\delta$  6.36 (1H, s), 6.86 (1H, s), 7.38 (1H, s)] (Fig. S1†). These were the characteristic mangiferin signals. The high field peak  $\delta$  4.59 (d, 9.8 Hz) was the core mangiferin glucose terminal hydrogen signal. The  $\delta$  73.1 ppm methylene may be  $\beta$ -sugar terminal carbon, which was connected with C–C bond. The  $\delta$  104.2 ppm quaternary carbon should be the other sugar terminal carbon (Fig. S2†). HSQC spectra can classify all the carbon signals except the quaternary carbon (Fig. S4†). The connections of each self-spinning



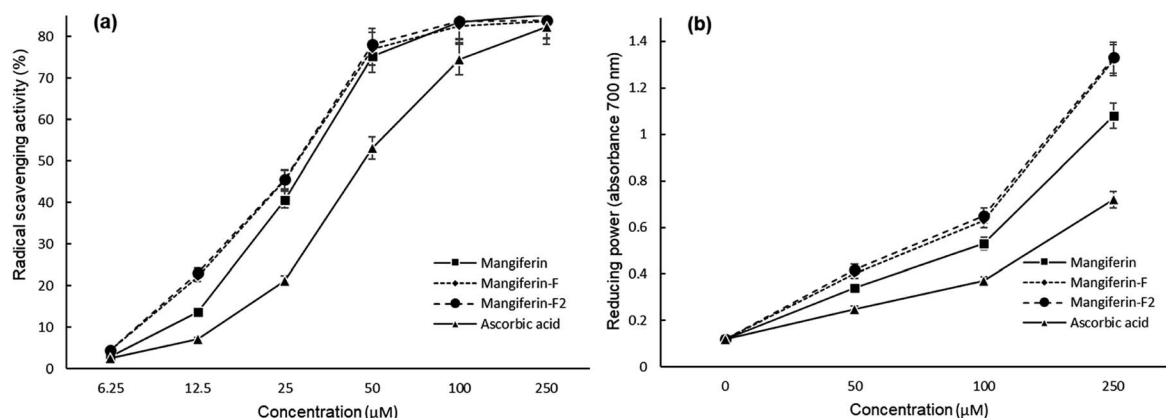


Fig. 3 Antioxidant activity mangiferin and its glycosides. (a) DPPH scavenging effect; (b) reducing power.

segment can be inferred by HMBC spectra. From the  $^{13}\text{C}$ -NMR,  $^1\text{H}$ -NMR and 2D NMR spectra, the monosaccharide was identified as  $\beta$ -D-fructofuranose. The other diagnostic difference between compound **II** and mangiferin was the carbon signal at C-6' of the glucose moiety, which was about 0.9 ppm downfield from those of mangiferin due to the known effects of *O*-glycosylation. Moreover, the carbon signal of C-5' was about 6.3 ppm upfield from that of mangiferin. The HMBC spectrum showed long-range correlations between C-2'' ( $\delta_{\text{C}}$  104.2) and H-6' ( $\delta_{\text{H}}$  3.42, 3.52) of glucose moiety and H-1'' ( $\delta_{\text{H}}$  3.30–3.40) of fructose moiety, thus proving the correlation between C-2'' and H-6' of compound **II** (Fig. S5†). Therefore, the chemical structure of compound **II** was elucidated as  $\beta$ -D-fructofuranosyl-(2  $\rightarrow$  6)-mangiferin. The high-resolution ESI mass spectrum of compounds **III** showed an ion peak  $[\text{M}-\text{H}]^-$  at  $m/z$  745.1813 (calculated for  $\text{C}_{31}\text{H}_{37}\text{O}_{21}$ , 745.1827) (Fig. S11-b†). Compared with mangiferin, the compound **III** has an additional formula  $\text{C}_{12}\text{H}_{20}\text{O}_{10}$ , suggesting that compound **III** may be a mangiferin disaccharide derivative. The  $\delta$  73.2 ppm methylene should be  $\beta$ -sugar terminal carbon, which was connected with C–C bond. The  $\delta$  104.3 ppm and 104.2 ppm quaternary carbon should be fructose terminal carbon (Fig. S7†). The other diagnostic difference between compound **III** and mangiferin was the carbon signal at C-6' ( $\delta_{\text{C}}$  62.9) of the glucose moiety, which was about 1.4 ppm downfield from those of mangiferin due to the known effects of *O*-glycosylation. And the carbon signal at C-6'' ( $\delta_{\text{C}}$  62.5) was about 0.6 ppm downfield from those of compound **II**. The HMBC spectrum showed long-range correlations between C-2'' ( $\delta_{\text{C}}$  104.3) and H-6' ( $\delta_{\text{H}}$  3.51, 3.72) of glucose moiety and H-1'' ( $\delta_{\text{H}}$  3.28–3.40) of fructose moiety, thus proving the correlation between C-2'' and H-6' of compound **III** (Fig. S10†). The HMBC spectrum also showed long-range correlations between C-2''' ( $\delta_{\text{C}}$  104.2) and H-6'' ( $\delta_{\text{H}}$  3.42, 3.51) of fructose moiety and H-1''' ( $\delta_{\text{H}}$  3.26–3.37) of fructose moiety, thus proving the correlation between C-2''' and H-6'' of compound **III** (Fig. S10†). Therefore, the chemical structure of compound **III** was elucidated as  $\beta$ -D-difructofuranosyl-(2  $\rightarrow$  6)-mangiferin. The spectroscopic data for  $^1\text{H}$  and  $^{13}\text{C}$ -NMR (500 MHz,  $\text{DMSO}-d_6$ ) were summarized in Table 2.

### 3.3 Antioxidant activity

The DPPH scavenging potential of mangiferin, mangiferin-F, mangiferin-F2 and ascorbic acid at different concentrations is shown in Fig. 3a. Significant DPPH radical scavenging activity was evident at 50  $\mu\text{M}$  concentration of mangiferin (75.2%), mangiferin-F (77.1%), mangiferin-F2 (78.1%) and ascorbic acid (53.1%). The scavenging effect of mangiferin glycosides were higher than that of mangiferin and ascorbic acid. Fig. 3b shows the reducing powers of different concentrations of mangiferin, mangiferin-F, mangiferin-F2 and ascorbic acid using potassium ferricyanide reduction method. The reducing power of four samples correlated well with increasing concentrations. Moreover, the reducing power of mangiferin glycosides was relatively more pronounced than that of mangiferin and ascorbic acid. DPPH scavenging effect and reducing power of mangiferin glycosides suggests that glycosylation of mangiferin increases the antioxidant activities to a certain extent.

### 3.4 Cytotoxicity assay

MTT assay was performed to compare the cell cytotoxicity induced between mangiferin and its glycosides. As shown in Table 3, mangiferin showed effective cytotoxicity on TPC1 cells ( $\text{IC}_{50}$  4.2  $\mu\text{M}$ ) and HL60 cells ( $\text{IC}_{50}$  72.8  $\mu\text{M}$ ) after 48 h of incubation. The cytotoxicity of mangiferin glycosides were better than that of mangiferin, mangiferin-F presented  $\text{IC}_{50}$  values of 3.8 and 65.8  $\mu\text{M}$  for TPC1 and HL60 tumor cell lines, respectively. However, there no obvious difference of antitumor activity between mangiferin-F and mangiferin-F2. This suggests that glycosylation of mangiferin can enhances the antitumor activity.

Table 3 The cytotoxicity activity of mangiferin and its glycosides

Cells	$\text{IC}_{50}$ (Mean $\pm$ SD, $\mu\text{M}$ )		
	Mangiferin	Mangiferin-F	Mangiferin-F2
TPC1	4.2 $\pm$ 0.4	3.8 $\pm$ 0.3	3.7 $\pm$ 0.5
HL60	72.8 $\pm$ 2.9	65.8 $\pm$ 1.7	65.2 $\pm$ 2.1



## 4. Conclusions

In summary, a HSCCC method was successfully established to separate and purify mangiferin and its glycosides. Two mangiferin glycosides were obtained in one-step isolation, and their purities were more than 98.7%. The DPPH scavenging activity and reducing power analysis demonstrated that  $\beta$ -D-fructofuranosyl-(2  $\rightarrow$  6)-mangiferin and  $\beta$ -D-diffructofuranosyl-(2  $\rightarrow$  6)-mangiferin showed better antioxidant activities than that of mangiferin. The cytotoxicity of two mangiferin glycosides were also better than that of mangiferin,  $\beta$ -D-fructofuranosyl-(2  $\rightarrow$  6)-mangiferin presented IC<sub>50</sub> values of 3.8 and 65.8  $\mu$ M for TPC1 and HL60 tumor cell lines, respectively.

## Conflicts of interest

All authors declare no conflicts of interest.

## Acknowledgements

This project was sponsored by National Key R&G Program of China (2018YFC1706201), Natural Science Foundation of Jiangsu (BK20161038), and PAPD.

## References

- 1 K. Sanugul, T. Akao, Y. Li, N. Kakiuchi, N. Nakamura and M. Hattori, *Biol. Pharm. Bull.*, 2005, **28**, 1672–1678.
- 2 S. Jaiswal, K. Ramesh, G. Kapusetti, A. K. Ray, B. Ray and N. Misra, *Polym. Bull.*, 2015, **72**, 1407–1416.
- 3 R. Boonnattakorn, V. Chonhenchob, M. Siddiq and S. P. Singh, *Packag. Technol. Sci.*, 2015, **28**, 241–252.
- 4 P. K. Jain, K. Kumar and A. Gajbhiye, *Drug Dev. Ind. Pharm.*, 2013, **39**, 1840–1850.
- 5 J. J. Jeong, S. E. Jang, S. R. Hyam, M. J. Han and D. H. Kim, *Eur. J. Pharmacol.*, 2014, **740**, 652–661.
- 6 B. B. Garrido-Suárez, G. Garrido, M. E. García and R. Delgado-Hernández, *Phytother. Res.*, 2014, **28**, 1646–1653.
- 7 F. Gold-Smith, A. Fernandez and K. Bishop, *Nutrients*, 2016, **8**, 396–421.
- 8 J. Hou, D. L. Zheng, F. Gabriel, H. Y. Deng, L. Chen, J. L. Liang, Y. Jiang and Y. H. Hu, *Can. J. Physiol. Pharmacol.*, 2015, **94**, 332–340.
- 9 Y. P. Zhao, W. H. Wang, X. H. Wu, X. Q. Ma, R. Z. Qu, X. M. Chen, C. H. Liu, Y. G. Liu, X. K. Wang, P. C. Yan, H. Zhang, J. R. Pan and W. W. Li, *Int. Immunopharmacol.*, 2017, **45**, 174–179.
- 10 I. Gill and R. Valivety, *Angew. Chem., Int. Ed.*, 2000, **39**, 3804–3808.
- 11 C. G. Yu, H. D. Xu, G. D. Huang, T. Chen, G. Y. Liu, N. Chai, Y. Ji, S. Y. Wang, Y. J. Dai and S. Yuan, *Appl. Microbiol. Biotechnol.*, 2010, **86**, 863–870.
- 12 X. M. Wu, J. L. Chu, B. Wu, S. Zhang and B. F. He, *Bioresour. Technol.*, 2013, **129**, 659–662.
- 13 X. M. Wu, J. L. Chu, J. Y. Liang and B. F. He, *RSC Adv.*, 2013, **3**, 19027–19032.
- 14 D. J. Wang, X. Y. Song, H. J. Yan, M. M. Guo, R. M. Fu, H. L. Jiang, H. Zhu and X. Wang, *RSC Adv.*, 2018, **8**, 34321–34330.
- 15 D. J. Wang, M. S. Khan, L. Cui, X. Y. Song, H. Zhu, T. Y. Ma and R. Sun, *RSC Adv.*, 2019, **9**, 4892–4899.
- 16 J. Q. Yu, X. W. Sun, L. Zhao, X. Y. Wang and X. Wang, *RSC Adv.*, 2020, **10**, 11132–11138.
- 17 D. Q. Li, J. Zhao, D. Wu and S. P. Li, *J. Chromatogr. B: Anal. Technol. Biomed. Life Sci.*, 2016, **1021**, 81–90.
- 18 F. Luo, Q. Lv, Y. Zhao, G. Hu, G. Huang, J. Zhang, C. Sun, X. Li and K. Chen, *Int. J. Mol. Sci.*, 2012, **13**, 11260–11274.
- 19 J. He, P. Fan, S. Feng, P. Shao and P. Sun, *Molecules*, 2018, **23**, 560.
- 20 B. Chen, Y. Peng, X. Wang, Z. Li and Y. Sun, *Molecules*, 2017, **22**, 2002.
- 21 N. Singh and P. S. Rajini, *Food Chem.*, 2004, **85**, 611–616.
- 22 G. K. Jayaprakasha, R. P. Singh and K. K. Sakariah, *Food Chem.*, 2001, **73**, 285–290.
- 23 L. Zhang and M. C. Wang, *Biotechnol. Bioprocess.*, 2018, **23**, 649–654.
- 24 Y. Ito, *J. Chromatogr. A*, 2005, **1065**, 145–168.
- 25 X. M. Wu, J. L. Chu, T. T. Xu and B. F. He, *J. Chromatogr. B: Anal. Technol. Biomed. Life Sci.*, 2013, **935**, 70–74.

